DOI: 10.21062/mft.2026.035 http://www.journalmt.com

Gradient Stiffness Modelling of Thin Adhesive Bonds

Kamil Anasiewicz (0000-0001-8728-236X)
Faculty of Mechanical Engineering, Lublin University of Technology. Nadbystrzycka st. 36, 20-618 Lublin. Poland.
E-mail: k.anasiewicz@pollub.pl

The objective of this study was to evaluate the influence of through-thickness variability of Young's modulus on the numerical modelling of adhesive joint behaviour. The study combined experimental characterization with finite element simulations. Nanoindentation measurements were used to determine the distribution of Young's modulus across adhesive layers with thicknesses of 0.05 mm and 0.1 mm. Based on these measurements, two-dimensional finite element models of double-overlap joints were developed in Abaqus. Two modelling approaches were analysed: a conventional homogeneous model with constant material properties and a heterogeneous multi-zone model in which Young's modulus varies across the adhesive thickness and is implemented using the USDFLD user subroutine. The results indicate that incorporating experimentally determined stiffness gradients significantly alters the predicted stress field, particularly in regions near the overlap ends where failure initiation is expected. The heterogeneous model provides improved agreement between numerical predictions and experimentally determined failure stresses. These findings demonstrate that accounting for stiffness heterogeneity improves the accuracy of numerical modelling of ultra-thin adhesive joints.

Keywords: Adhesive bonding, Apparent Young's modulus, Heterogeneity of adhesive joints, FEM

1 Introduction

Numerical modelling plays a key role in materials engineering, enabling the prediction of structural integrity of materials and joints in a wide range of applications from aerospace to automotive. Traditional finite element methods (FEM) and cohesive zone modelling (CZM) are readily used to simulate stress distributions, failure modes, and nonlinear material responses in adhesive bonds. The following introduction synthesizes key research on the modelling of adhesive joint strength, with an emphasis on nonlinear behaviours such as inhomogeneities and property gradients in the adhesive layer. Particular emphasis has been placed on models that take into account property variations, such as the Young's modulus gradient - higher near the substrate-adhesive interface and decreasing toward the core of the joint. The discussed work provides a basis for developing advanced material models that take these gradients into account, addressing the limitations of the homogeneity assumptions for adhesive joints.

The literature contains many studies dedicated to explaining the critical factors affecting the reliability and integrity of adhesive bonds. The stiffness of the bonded materials is a very important factor affecting the strength of the adhesive bond. Young's modulus defines the characteristic relationship between the relative linear deformation ε of a material and the stress σ occurring in it within the range of elastic deformation [1]. One of the popular methods for determining the Young's modulus of materials, in this case adhesive, is the axial tensile testing of cast adhesive samples. The samples are standardized and have a paddle shape [2]. A properly prepared sample is placed in the jaws of a testing machine. In order to obtain the most accurate σ-ε relationship, an extensometer is used to measure the elongation of the sample over the accepted measurement section. The test results in the σ-ε characteristic, on the basis of which the Young's modulus of the adhesive material can be determined. However, it should be emphasized that this is the Young's modulus of the adhesive material and may differ from the Young's modulus in the adhesive joint. Kinloch [3] provides a definition of the apparent Young's modulus, defined as the ratio between the applied shear stress and the deformation at the thickness of the adhesive joint, which is greater than the actual Young's modulus of the adhesive joint. The increased value of the Young's modulus is based on the assumption that the adhesive material in the adhesive joint is strongly bonded to the substrate of the rigid joint material.

Construction adhesives achieving a Poisson's ratio of 0.35 according to literature data means that the adhesive in the adhesive joint could have a Young's modulus value up to 60% higher than the Young's modulus value of the adhesive material [3,4]. However, the issues discussed by Kinloch do not take into account the relationship between the apparent Young's modulus and the thickness of the adhesive

joint, specifically the dependence of changes in the adhesive joint on the distance from the phase boundary and potential changes in the Poisson's ratio. It should also be taken into account that the thickness of joints in adhesive bonds is usually small, so assuming their ideal stiffness is a significant simplification.

Researchers have often analyzed the effect of adhesive bond thickness on the strength of lap and double-overlap joints using analytical calculations and the finite element method, demonstrating an increase in maximum strength for "flexible" adhesives as thickness decreases [5,6,7,8]. This comparison is difficult due to the complex adhesive and cohesive interactions in the bond [1,9]. To intensify the cohesive interaction, samples were used as a stack of alternately bonded butt joints, destroyed with an extensometer and compared with paddle samples, which indicated slight differences in Young's modulus and the influence of the bonded material on changes in joint properties during curing [7]. In [10], the authors analyzed the effect of bond thickness on composite angle joints, concluding that the destructive stress decreases with increasing thickness, with a flat stress state for thin adhesive joints and flat deformation for thicker ones, emphasizing that the differences in strength result from stress states rather than material properties, which allows the use of data from paddle samples in design (for thicknesses of 0.25–2.5 mm). Subsequent studies examined aluminum substrates with epoxy adhesives of various thicknesses, noting a deterioration in mechanical properties with increasing thickness, explained by a change in stress state in numerical analyses [11]. In summary, the strength of adhesive joints increases with decreasing thickness [12,13], although for "thick" lap joints, the destructive load initially increases (0.15–0.45 mm) and then decreases (0.9 mm), with a trend of degradation in butt joints attributed to reinforcement in a smaller volume and fewer defects. Lee et al. show that in elastomer-modified epoxies, the material properties in the fracture zone vary locally, which affects fracture resistance. The authors emphasize the existence of heterogeneous stiffness gradients near the fracture tip, which is important for accurate adhesive joint modelling [14]. Adams and Coppendale show that the stiffness of the adhesive joints significantly affects the actual stress-strain characteristics in butt joints. Restrictions on movement caused by stiff joints result in an apparent increase in the Young's modulus of the adhesive joint [15]. Studies of thin coatings have shown higher hardness (correlated with Young's modulus) for thinner layers, decreasing with increasing thickness of the coating layer [16]. To summarize the presented studies, it can be concluded that the phenomenon described as the apparent Young's modulus of an adhesive joint is strictly dependent on the thickness of the joint, the stiffness of the adhesive, the configuration of the joint, and even the method of use of the adhesive joint [8]. All the research studies presented so far should certainly be analyzed in terms of the phenomena occurring in the joint during the formation of the adhesive connection, phenomena related to adhesion, and the interaction of the surfaces of the joined elements with the adhesive in its liquid state. The results of the studies presented often indicated discrepancies in the strength of the adhesive joint in relation to the strength of the adhesive material. However, these differences were closely correlated with the thickness of the adhesive layer as well as material of the joints.

In the case of adhesive joints, determining the correct values for Young's modulus or Poisson's ratio of the cured adhesive can be a complex but very important problem. Adhesive in a liquid state, which is in contact with a metal surface with a highly developed surface area, is subjected to physisorption and chemisorption forces at the phase boundary. In addition, due to the high heat capacity of metal, it strongly absorbs heat from the curing adhesive, and this reaction is usually exothermic. This can have a direct effect in the form of differences in the physical properties of the adhesive, including cross-linking density and a certain "ordering" of the structure in chemically curable adhesives in the area located in the phase boundary zone compared to the material in the center of the joint. The cross-link density of epoxy resin has a direct impact on the properties of the adhesive and affects its stiffness and strength. In contrast to the paddle sample, in thin joints, the adhesive cures in the presence of the energetic interaction of rigid joint elements and varying thermal curing conditions in the wall and center zones of the joint. This leads to a complex stress state in the loaded joint as a result of changes in the cross-sectional structure of the joint [18-20]. Physical adsorption causes the substance (adhesive) to condense on the surface of the adsorbent, which occurs due to intermolecular attractive forces. This interaction causes a specific ordering of the adhesive structure in the wall (interphase) zone, which is in direct contact with the bonded surface. These phenomena, interacting with the epoxy resin particles, cause their concentration [21]. The consequences of these phenomena are called apparent Young's modulus E'. In certain applications and adhesive joint thicknesses, these changes can cause errors in the design of adhesive joints and inaccuracies in the calculation of their strength.

Analytical models of adhesive bonds play an important role in predicting stress and strain distributions, often relying on maximum values as failure criteria, although they require extensive

ISSN 1213–2489
e-ISSN 2787–9402

experimental testing for specific material combinations [22]. Most of these models introduce simplifications, such as linear adhesive joint characteristics or limitations to specific geometries and materials, which facilitate calculations but limit their versatility [23]. In terms of numerical modelling, these analytical approaches can serve as a reference point for validating FEM simulations, although they are not the dominant part of contemporary literature reviews, where numerical methods such as CZM prevail. Volkersen's model ignores bending effects, focusing on shear stresses τ in the joint, expressed by a formula that takes into account the overlap geometry and material moduli, which emphasizes the uneven stress distribution with maxima at the ends of the overlap. Goland and Reissner [24] took into account the deformations of the joined elements, dividing the problem into the determination of edge loads and stresses, which allows for the calculation of both τ and σ tearoff stresses, with lower maximum values compared to Volkersen in the absence of moments [25]. The Hart-Smith model [26] introduces nonlinearity through the plasticity of the adhesive, analyzing single and double joints with the lap divided into elastic and plastic zones, which allows for the inclusion of bi-linear elastic-plastic characteristics in strength predictions. Despite their simplifications, these analytical models aid in understanding the influence of the Young's modulus gradient on stress distribution, although in numerical simulations they integrate better with advanced tools such as user subroutines in Abaqus. In summary, although analytical models remain useful for quick estimates, their role in modelling is complementary to the dominant numerical methods.

Kalina and Sedláček [27] presented a comprehensive methodology for combining mathematical models with FEM analysis and experimental results, showing that the accuracy of predicting the strength of adhesive bonds increases significantly when nonlinear failure mechanisms and material inhomogeneities are taken into account. The authors point out that local differences in properties, including Young's modulus variability, can have a key impact on crack initiation, which fits well into the concept of joints with gradient stiffness. Kolář [28] analyzed the effect of recycled additives on the microstructure and behavior of polyurethanes, showing that modifications in composition lead to local changes in cross-linking and hardness, which in thin joints can translate into heterogeneous stiffness profiles and requires representation in numerical modeling. In studies on degradation and fatigue, Müller [29], Šleger et. al. [30], and Cidlina et. al. [31] have shown that chemical aging, the interaction of processing fluids, and cyclic loading lead to a varied loss of properties in the bond. This is important for Young's modulus modelling, because a real bond does not degrade uniformly, and changes in stiffness can increase over time, requiring inclusion in FEM through variable material fields. On the other hand, Corrado et. al. [32] showed that assembly errors and misalignment of connections can strongly amplify local stress concentrations, which are further intensified in the presence of a stiffness gradient - making his model useful for parametric analyses combining assembly tolerances with Young's modulus. The most direct contribution to the development of the variable stiffness model, which uses nanoscratching to assess local homogeneity and shows clear differences in properties across the adhesive joint cross-section. These data provide an empirical basis for calibrating the E function, confirming the actual presence of zones of increased and decreased stiffness, which directly enables the verification of a numerical model of an adhesive bond with variable properties [33].

The review emphasizes that most research on adhesive joints focuses on joint strength, surface preparation, and stress simulations, while the properties of the joint itself and their variability across thickness are analyzed much less frequently. Although the influence of joint thickness on strength is widely described, very thin joints below 0.1 mm, in which strengthening and apparent Young's modulus phenomena occur, are almost completely ignored. Current numerical methods, including CZM and XFEM, typically do not take into account property gradients, and analytical models describe variability along the lap but not across the bond thickness. The apparent Young's modulus phenomenon depends on the material, bond thickness, and operating conditions, and its omission leads to inaccuracies in the modelling of thin joints. Therefore, there is a need for further research and development of models that can reproduce the actual stiffness gradients of bonds, calibrated experimentally, in order to increase the accuracy of FEM analyses. In contrast to previous investigations focused primarily on the influence of adhesive thickness on global joint strength, the present study isolates the role of experimentally quantified through-thickness stiffness gradients on local stress concentration mechanisms. The objective is not only to compare homogeneous and heterogeneous material representations, but to determine whether the inclusion of a physically measured stiffness profile alters the predicted failure-driving stress field in a statistically significant manner. This distinction is essential because failure in thin adhesive joints is governed by highly localized stress peaks rather than by global stiffness effects alone.

2 Methodology

The experiment used the results of nanoindentation tests, which provide information on the distribution of Young's modulus values across the thickness of the adhesive joint. The tests were conducted for two joint thicknesses, i.e., 0.05 mm and 0.1 mm. The results of these tests were used as input data for the development of a numerical model of an adhesive bond with variable stiffness [34]. In order to verify the numerical tests, adhesive bond samples were prepared in an analogous manner. Double-overlap specimens according to ASTM D3528 were selected for the stress testing of adhesive joints. These are specimens with four adhesive joints of equal lap length. Double-overlap specimens are characterized by symmetrical loading in all joints due to the design of the specimen and the method of loading. In this test, the average elongation values at failure of the adhesive joint were determined. These values were used as data for numerical calculations. The tests were carried out for two epoxy adhesives, namely Epidian 57/PAC – referred to as "flexible" and Epidian 57/Z1 – referred to as "rigid" [35-37]. A tensile test of the adhesive material in the form of a paddle was carried out in accordance with DIN EN ISO 527-1 [2]. In this test, the strength of the adhesive material was determined. Based on the obtained tensile curves, the Young's modulus values of the adhesive materials were calculated.

Double-overlap specimens for tensile testing were made of EN AW-2024 T3 aluminum alloy, using 9.15 mm thick connectors and 4.56 mm thick overlays, cut with high precision using hydroabrasion. The connectors were milled as panel elements, with a separating groove and positioning holes, which allowed for precise positioning of the overlays and maintaining a constant overlap length. The surfaces intended for bonding were prepared in the same way as in the butt samples for nanoindentation testing, and the adhesive composition was applied manually, removing any excess. A silicone insert was placed in the groove to prevent the space from being filled with adhesive, and a constant joint thickness was ensured by means of steel spacers (0.05 mm and 0.1 mm). Similar to the samples in the nanoindentation tests, adhesive joints were prepared in two variants of adhesive joint thickness, i.e., 0.05 mm and 0.1 mm. The assembled elements were cured in a vacuum bag under a pressure of 0.1 MPa for 24 hours, and then seasoned for a minimum of 168 hours. The final samples were cut from the panel with a hydroabrasive jet, which ensured the integrity of the adhesive joint. The milled samples, prepared for bonding, are shown in Fig. 1.

The Young's modulus of the adhesive was determined in an axial tensile test on paddle samples made of a cured adhesive composition. The adhesive mixture was prepared in the proportions recommended by the manufacturer, then cast in silicone moulds, and after 168 hours of curing, the samples were milled to a thickness of 4 mm. They were then subjected to a static tensile test in accordance with DIN EN ISO 527-1, using an extensometer to precisely measure deformations over a 50 mm section. The aim of the test was to determine the modulus of elasticity in the proportional range.

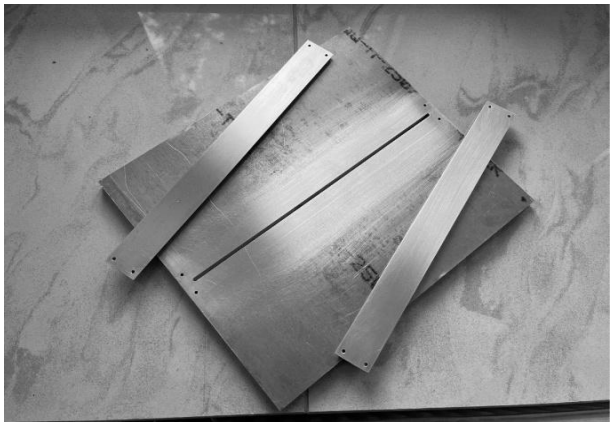

Fig. 1 *Samples in the form of a panel prepared for adhesive bonding, with a visible groove and positioning holes*

Based on the results obtained from the experiment, a numerical model was prepared in the Abaqus program. The aim of the study is to compare the stress state in the adhesive joint in a model that takes into account the variation in material properties across the thickness of the joint and in a model with homogeneous properties throughout the entire volume of the adhesive joint. In order to define the significance of differences in Young's modulus values across the adhesive joint thickness, a numerical model was constructed taking into account the changed Young's modulus values obtained in the nanoindentation test. A double-overlap sample in 2D representation in two variants, with dimensions compliant with ASTM D3528, was selected for verification. In the first variant, adhesive joints with a thickness of 0.05 mm and 0.1 mm were presented as single-zone joints with the same Young's modulus value of the adhesive joint throughout the entire volume of the adhesive joint. In the second variant, the Young's modulus of the joint was changed as a function of the joint thickness by using a subroutine.

The selection of adhesive layer thicknesses of 0.05 mm and 0.1 mm was not arbitrary. These values correspond to the range of ultra-thin adhesive joints commonly encountered in high-performance structural applications, where the constraint effect imposed by the adherends is most pronounced. Previous studies have shown that below approximately 0.1 mm, the apparent Young's modulus

effect becomes significant due to restricted lateral deformation of the adhesive layer. The chosen thicknesses therefore represent a critical range in which through-thickness stiffness gradients are expected to have the strongest influence on stress distribution and failure initiation. The objective of this study is not to establish a general thickness-dependent model, but to investigate the local effect of experimentally measured stiffness gradients within this critical thickness range.

When developing adhesive joint models for the purpose of simulating adhesive joint stress, various modelling options were considered. One option was to divide the adhesive joint along its thickness into separate solids for which the modified joint properties could be defined independently. In the case of adhesive joints, this modelling method can be problematic due to their very small thickness. It can often lead to the formation of stress singularities in the joint, caused by dividing the joint into increasingly smaller finite elements. In numerical modelling, the denser the MESH grid used at the point of load application, the closer the considered stress interaction area will be to zero. This means that each subsequent iteration will generate increasingly higher stress values, even though the value of the applied load does not change. This results in incorrect stress values at important points in the model geometry. The above is true when, for example, an adhesive bond with a thickness of 0.1 mm is divided into parts representing changes in the Young's modulus value across its thickness. Dividing it into smaller solids results in the need to divide them into at least 3 finite elements, which leads to excessive mesh density in the bond area. To verify numerical robustness, convergence was assessed not only in terms of peak stress magnitude but also with respect to stress gradient stability at the overlap end. The second derivative of the stress distribution along the overlap was monitored. Stabilization of both peak magnitude and gradient curvature confirmed that the adopted mesh density does not artificially amplify stress concentration. Fig. 2 shows the division of the adhesive joint into three solids, with a visible dense finite element mesh in the wall areas.

In order to reproduce the actual, experimentally confirmed variability of Young's modulus along the thickness of the adhesive bond, it is necessary to use a material description that goes beyond classic, homogeneous linear models. The introduction of heterogeneity in a physically justified manner requires the implementation of a material with variable field characteristics, which in the Abaqus environment can be achieved through user subroutines. This approach uses the USDFLD subroutine, which allows variable fields to be assigned at each integration point as a function of time, strain, stress, temperature, or other quantities available in the set of material variables. This mechanism allows for dynamic, iterative updating of material properties, including Young's modulus, based on local state variable values, making it a particularly useful tool for mapping property gradients in bonds. The use of USDFLD allows the local stiffness of the material to be coupled with the position of the point on the bond thickness, so that Young's modulus can be assigned as a function of the normal coordinate, consistent with the profile obtained from nanoindentation tests. The subroutine is called at each calculation step for all integration points of elements in which field variables controlling material characteristics are defined, which allows for continuous correction of properties during deformation and ensures consistency with the nonlinear solution process. The implementation of this procedure requires the appropriate configuration of the Abaqus computational environment to work with the Fortran compiler, which includes integration with MS Visual Studio, configuration of system paths, and modification of environment variables to enable correct compilation of subroutines. After the configuration, a USDFLD was developed that assigns a field variable determining the Young's modulus as a function of the thickness coordinate, which allowed the creation of a numerical model that accurately reflects the heterogeneous nature of the stiffness of the adhesive joint. Fig. 3 shows the subroutine used in the numerical calculations.

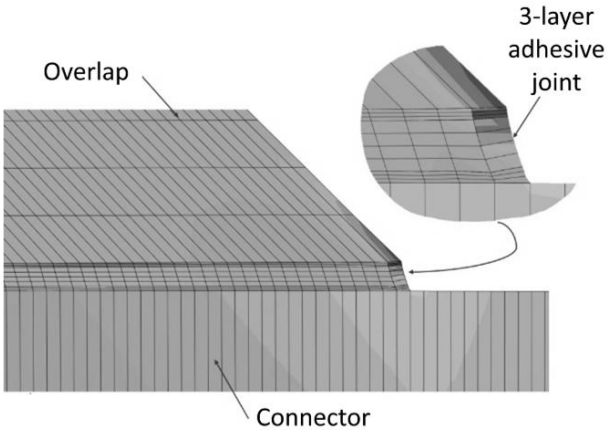

Fig. 2 *Division of the joint into three solids, with a visible dense finite element mesh in the wall-adjacent zones*

A numerical model of a double-overlap adhesive joint was developed in two dimensions, treating it as a plane strain state, which is a reasonable approach for thin geometries and allows for precise reconstruction of stress distributions along the lap. The model defined boundary conditions reflecting the loading in the testing machine: one of the connectors was immobilized by an *Encastre* condition, eliminating all degrees of translational and rotational freedom, while the other was subjected to an applied tensile load

corresponding to the loading conditions used in the experimental test. The connections and overlaps were made of EN AW-2024 T3 material, reproducing their actual geometry, including an overlap length of 12.7 mm. The adhesive joint was described by an elastic-plastic material whose σ(ε) characteristics were obtained experimentally.

```
SUBROUTINE USDFLD(FIELD,STATEV,PNEWDT,DIRECT,T,CELENT,
     1 TIME,DTIME,CMNAME,ORNAME,NFIELD,NSTATV,NOEL,NPT,LAYER,
     2 KSPT,KSTEP,KINC,NDI,NSHR,COORD,JMAC,JMATYP,MATLAYO,LACCFLA)

      INCLUDE 'ABA_PARAM.INC'

      CHARACTER*80 CMNAME, ORNAME
      CHARACTER*8 FLGRAY(15)
      DIMENSION FIELD(NFIELD),STATEV(NSTATV),DIRECT(3,3),
     1 T(3,3),TIME(2)
      DIMENSION ARRAY(15),JARRAY(15),JMAC(*),JMATYP(*),COORD(*)

C Variable declaration
      REAL THICKNESS, E_MODULUS
      INTEGER N, I

C N - number of nodes across the adhesive bond thickness
      N = STATEV(1)

C Dynamic determination of thickness and Young's modulus values
      REAL, DIMENSION(N) :: THICKNESS_TABLE, MODULUS_TABLE
      THICKNESS = COORD(2)

C Assignment of values to THICKNESS_TABLE and MODULUS_TABLE arrays
      DO I = 1, N
        THICKNESS_TABLE(I) = STATEV(1 + 2 * I)
        MODULUS_TABLE(I) = STATEV(2 + 2 * I)
      END DO

C *** Interpolation of Young's modulus value from the table ***
      IF (THICKNESS .LE. THICKNESS_TABLE(1)) THEN
        E_MODULUS = MODULUS_TABLE(1)
      ELSE IF (THICKNESS .GE. THICKNESS_TABLE(N)) THEN
        E_MODULUS = MODULUS_TABLE(N)
      ELSE
        DO I = 1, N-1
          IF (THICKNESS .GE. THICKNESS_TABLE(I) .AND. THICKNESS .LT. THICKNESS_TABLE(I+1)) THEN
            E_MODULUS = MODULUS_TABLE(I) +
     1 (MODULUS_TABLE(I+1) - MODULUS_TABLE(I)) /
     2 (THICKNESS_TABLE(I+1) - THICKNESS_TABLE(I)) *
     3 (THICKNESS - THICKNESS_TABLE(I))
            EXIT
          END IF
        END DO
      END IF

C Setting the Young's modulus value in the first field variable
      FIELD(1) = E_MODULUS

      RETURN
END
```

Fig. 3 *A subroutine used in numerical calculations that makes the Young's modulus values dependent on the thickness of the adhesive joint*

The influence of the adherend material was explicitly considered through the selection of EN AW-2024 T3 aluminium alloy, which is characterized by a much high Young's modulus relative to the adhesive layer. This choice is consistent with standard testing procedures and ensures a pronounced mechanical constraint imposed on the adhesive layer during loading. The stiffness mismatch between the adherends and the adhesive is a key factor governing the development of the apparent Young's modulus effect, as it restricts transverse deformation of the adhesive and alters the stress state within the bondline.

The material properties of the adherends were kept constant throughout all simulations in order to isolate the influence of through-thickness stiffness gradients within the adhesive layer. This approach allows for a controlled analysis in which variations in stress distribution can be directly attributed to the introduced material heterogeneity rather than to changes in global structural stiffness. The loading conditions were defined in accordance with ASTM D3528 for double-overlap joints, which ensures a predominantly symmetric stress state and minimizes bending effects. This standardized configuration is particularly suitable for investigating the intrinsic behaviour of adhesive layers, as it reduces the influence of geometric asymmetry and allows for a more direct assessment of material-related effects.

The interactions between the connections and the adhesive layer were formulated as surface-surface contact, with the use of *Tie* constraints ensuring full bonding of the surfaces and load transfer without relative displacement and penetration. The model was based on a volume mesh structure of CPE4R quadrilateral elements, equipped with integration reduction and suitable for deformation analysis while minimizing numerical errors. The mesh was refined in critical areas of the adhesive bond to improve the accuracy of stress and strain gradient mapping. The model construction process in the Abaqus environment included: defining geometry partitions, assigning materials, implementing appropriate contact interactions, and verifying mesh quality. It was also ensured that the local densification of elements within the bond did not lead to the formation of artificial singularities. The model prepared in this way enabled the analysis of the stress in a double-overlap adhesive joint under flat deformation conditions, taking into account both the deformation of the joints and the nonlinear behavior of the adhesive layer [1]. Table 1 presents the most important material constants used in the modelling.

Tab. 1 *Material constants used in the numerical model*

Element	Material	Bond thickness	Young's modulus (experimental) [GPa]	Poisson's ratio [-]	Fracture stress (experimental) [MPa]
Single-zone adhesive joint	Epidian 57/PAC	0.05	0.979	0.34	37.7
		0.1	0.979		
	Epidian 57/Z1	0.05	1.71	0.34	55
		0.1	1.71		
Multi-zone adhesive joint	Epidian 57/PAC	0.05	1.99-2.48	0.34	37.7
		0.1	0.98-2.48		
	Epidian 57/Z1	0.05	3.31-4.54	0.34	55
		0.1	1.71-4.54		
Connector material	EN-AW 2024	-	73,000	0.3	435

In modelling joints using multi-zone joints, a variable Young's modulus value was used across its thickness. The change in the Young's modulus of the adhesive along its thickness was described in accordance with the values obtained in nanoindentation tests for joints made with Epidian 57/PAC and Epidian 57/Z1 adhesives [34].

3 Results and discussion

Fig. 4 compares the average elongation at break for both adhesives analyzed in relation to the thickness of the bond in the adhesive joint. An adhesive joint with a 0.1 mm thick joint made with Epidian 57/PAC adhesive achieves an average elongation at break 41.3% greater than that of a joint with a 0.05 mm thick joint. In the case of the "rigid" adhesive Epidian 57/Z1, an adhesive joint with a thickness of 0.1 mm is characterized by an average elongation at break 6.3% greater than that of a joint with a thickness of 0.05 mm. Table 2 shows the average values of strength and elongation at failure of adhesive joints made with the analyzed adhesives.

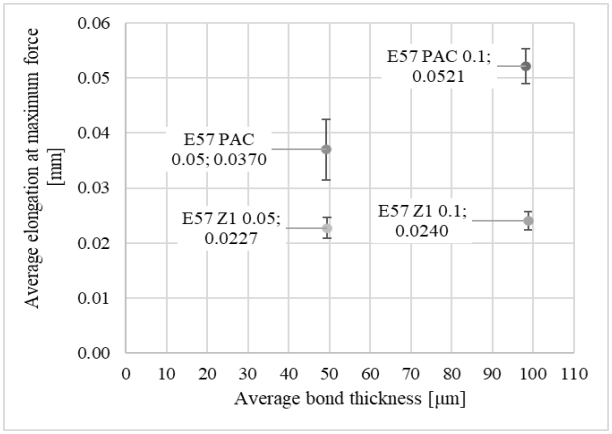

Fig. 4 *Comparison of average elongation values at the maximum force destroying the adhesive joint in relation to the average thickness of the adhesive joint*

Table 2 presents the results of the average strength of the adhesive material and Young's modulus, together with the standard deviation values, obtained experimentally in an axial tensile test of a paddle sample using an extensometer.

Tab. 2 *Average values of tensile strength and Young's modulus of adhesive materiál*

Adhesive	Average tensile strength [MPa]	Standard deviation [MPa]	Average Young's modulus [GPa]	Standard deviation [MPa]
Epidian 57/PAC	37.71	2.08	0.979	40.60
Epidian 57/Z1	56.08	2.14	1.701	20.73

In the FEM numerical model, following the multi-zone modelling approach, the adhesive layer was assigned spatially varying Young's modulus values across its thickness. These values were developed based on the results of experimental tests and adjusted to the thickness of the adhesive joints under consideration [34]. Fig. 5 and Fig. 6 show the changes in the Young's modulus values across the adhesive joint thickness for two thicknesses of the adhesive joints under consideration, which were used in the subprogram in the Abaqus software. Fig. 7 shows an example visualization of the deformation of a double-overlap adhesive joint with the finite element mesh density marked.

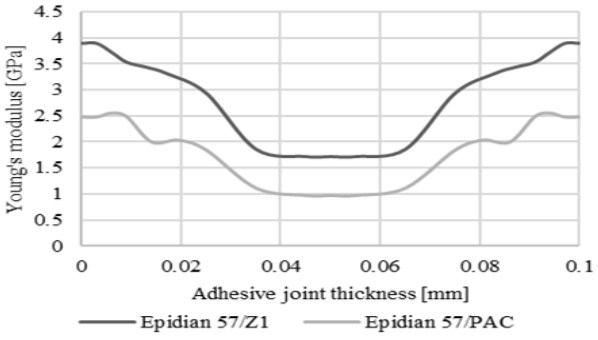

Fig. 5 *Changes in Young's modulus at a bonded joint thickness of 0.05 mm [34]*

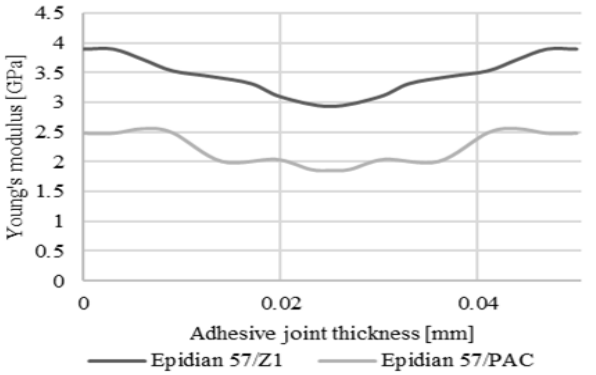

Fig. 6 *Changes in Young's modulus at a bond thickness of 0.1 mm [34]*

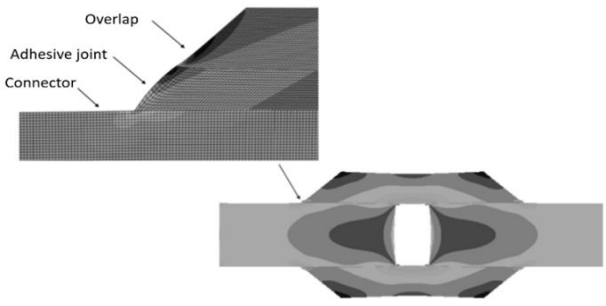

Fig. 7 *Visualization of the deformation of a double-overlap joint model with a representation of the finite element mesh density*

Figs. 8–11 show comparative graphs of reduced stress according to the Huber-Mises-Hencky hypothesis along a single lap of an adhesive joint. The graphs show differences in the maximum stress values at the end of the lap. In the multi-zone model, which reflects changes in the Young's modulus along the thickness of the adhesive joint, they are 7.4% higher than in the model with a uniform Young's modulus throughout the entire joint volume – the so-called 1-zone model, in the case of "rigid" adhesive Epidian 57/Z1 adhesive and a bond thickness of 0.1 mm.

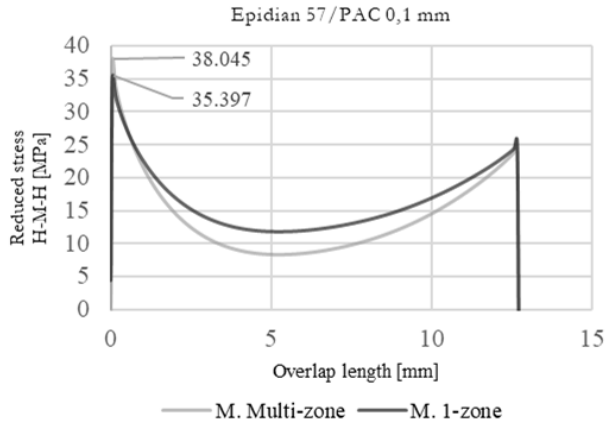

Fig. 8 *Reduced stresses in a 0.1 mm thick E57/PAC adhesive bond, along the lap for a 1-zone model and a multi-zone model taking into account changes in the Young's modulus value in the bond across its thickness*

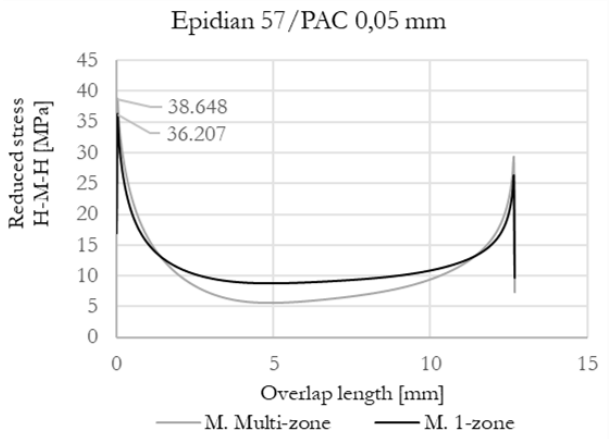

Fig. 9 *Reduced stresses in a 0.05 mm thick E57/PAC adhesive bond, along the lap for a 1-zone model and a multi-zone model taking into account changes in the Young's modulus value in the bond across its thickness*

In order to analyze the simulation results presented in the graphs below, it should be emphasized that the simulation modelled the stress on the adhesive joint until the joint failed. This means that it is possible to compare the stresses destroying the adhesive material with the reduced stresses in the adhesive joint subjected to deformation destroying the adhesive joint in the experimental test. Such a comparison will allow us to determine whether, at a given average deformation of the double-overlap specimen, a similar level of stress will be achieved in the joint material. Differences in stress values will indicate differences in the Young's modulus of the adhesive joint. Table 3 and Table 4 show a comparison of experimental results and simulation results for Epidian 57/PAC a nd Epidian 57/Z1 adhesives.

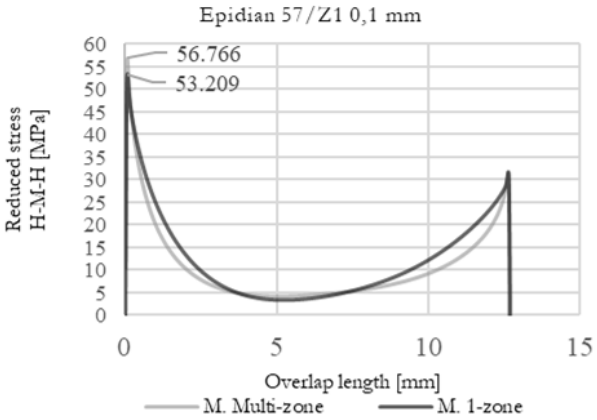

Fig. 10 *Reduced stresses in the E57/Z1 adhesive joint with a thickness of 0.1 mm, along the overlap for the 1-zone model and the multi-zone model taking into account changes in the Young's modulus in the joint across its thickness*

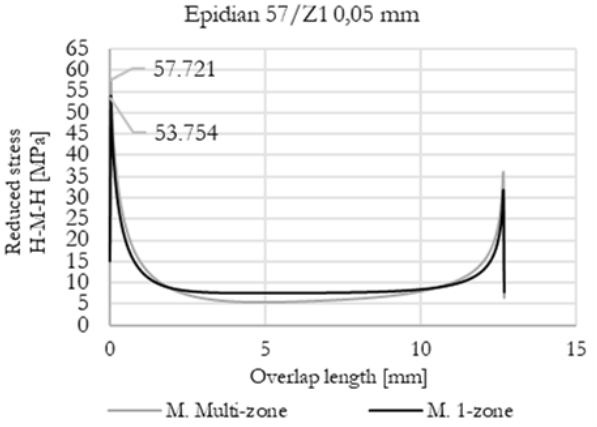

Fig. 11 *Reduced stresses in the E57/Z1 adhesive joint with a thickness of 0.05 mm, along the overlap for the 1-zone model and the multi-zone model taking into account changes in the Young's modulus value in the joint across its thickness*

The graphs shown in Fig. 8–Fig. 11 show the differences in reduced stress values according to the Huber-Mises-Henky hypothesis along the adhesive joint overlap in an adhesive joint. The graphs compare the stresses for two numerical models, one of which can be described as classic – single-zone, i.e., one that does not take into account the heterogeneity in the Young's modulus properties of the adhesive in the joint, and the other model, referred to here as a multi-zone (multi-layer) model, in which the value of

Young's modulus varies as a function of the thickness of the adhesive joint. It should be noted that the stress values shown in the graphs are values at the nodes located at the edge of the adhesive joint at the point of contact with the connection material. At the same time, this is the place where the highest reduced stresses were observed. Due to the similarity in the preparation of the analyzed numerical models, the outline of the stress curves is also similar. A significant difference is the value of reduced stresses at the ends of the overlap, i.e., in places where the initiation of adhesive joint failure is expected. When comparing the values of reduced stresses at the nodes located at the edge of the joint, the differences between the models are greater.

Tab. 3 *Comparison of experimental stress values and simulation results for Epidian 57/PAC adhesive*

Adhesive strength [MPa]	Model type	Adhesive joint thickness [mm]	Max. reduced stress in the joint [MPa]	Difference % relative to adhesive strength
37.708	single zone	0.05	36.207	-4.15
		0.1	35.397	-6.53%
	multi-zone	0.05	38.648	2.43
		0.1	38.045	0.89

Tab. 4 *Comparison of experimental stress values and simulation results for Epidian 57/Z1 adhesive*

Adhesive strength [MPa]	Model type	Adhesive joint thickness [mm]	Max. reduced stress in the joint [MPa]	Difference % relative to adhesive strength
56.075	single zone	0.05	53.754	-4.32%
		0.1	53.209	-5.39%
	multi-zone	0.05	57.721	2.85%
		0.1	56.766	1.22%

The results obtained in this study are consistent with contemporary research on the mechanical behaviour and numerical modelling of adhesive joints. Previous investigations have shown that the mechanical response of adhesive joints strongly depends on the stiffness of the adhesive layer and its interaction with the joined materials, which significantly influences the stress distribution and failure mechanisms in the adhesive bondline [38,39]. In particular, several studies indicate that simplified homogeneous material models may lead to discrepancies between numerical predictions and experimental results, especially in the case of very thin adhesive layers where the constraint imposed by the adherends modifies the effective stiffness of the adhesive bond [7]. The results presented in this work confirm that introducing spatial variability of Young's modulus across the adhesive thickness improves the agreement between numerical predictions and experimental observations. Similar conclusions have been reported in recent modelling studies, where the mechanical response of adhesive joints was shown to depend not only on the bulk properties of the adhesive but also on local variations of stiffness and stress concentration mechanisms occurring near the interfaces [39]. The present analysis further demonstrates that stiffness gradients primarily influence local stress peaks at the overlap edges, which are known to be the most critical regions for crack initiation in bonded joints. This observation is consistent with the general understanding that adhesive joints are highly sensitive to peel and normal stresses near the ends of the overlap, even when the overall stress distribution along the joint appears relatively uniform [40]. Consequently, the incorporation of experimentally calibrated stiffness gradients into finite element models can significantly improve the predictive capability of numerical simulations without the need to introduce more complex fracture or damage models. These findings highlight the importance of considering through-thickness material heterogeneity in the modelling of ultra-thin adhesive bonds.

Beyond the comparison of reduced von Mises stress values, a detailed overview of stress components was performed. The gradient model exhibits a measurable increase in peel stress (σ_y) near the overlap ends, while shear stress (τ_{xy}) distribution remains only moderately affected. This indicates that stiffness heterogeneity primarily amplifies normal stress components responsible for crack initiation at the interface. In contrast, the homogeneous model distributes deformation more uniformly, which reduces the maximum peel stresses and consequently postpones the predicted initiation of failure.

As the numerical model was developed to replicate the actual paddle specimen used in the axial tensile test as accurately as possible, the destructive stress values

could be compared at the same traverse displacement. The comparison can also be described as validation of the numerical model with the results of the actual test. The traverse displacement should be understood as the mutual displacement of the double-overlap joint connections over a distance of 50 mm, i.e., the distance over which the extensometer is placed. A direct comparison of the reduced stresses in the adhesive joint for both numerical models and the stresses calculated on the basis of the axial tensile test shows that the maximum stresses in the joint obtained in the simulation using the multi-zone model are closer to the actual stresses than those obtained using the classical model. The higher stresses occurring at the overlap edges in the multi-zone model, reaching values associated with failure, suggest an earlier onset of joint damage. From the perspective of damage mechanics, it should also be emphasized that the propagation of damage within the joint is constrained by the wall regions as a result of the heterogeneous structure of the adhesive layer. As a result, stresses increase in this region and owing to the enhanced strength provided by higher Young's modulus, adhesive failure of the bonded joint subsequently occurs.

4 Conclusions

Based on the presented results, it can be observed that the results of stresses destroying the adhesive material better match the results of reduced stresses according to H-M-H obtained in numerical calculations using a multi-zone model, which is intended to better reflect the behavior of an adhesive joint under load. The reduced stresses according to the H-M-H hypothesis and their highest level are observed at the edge of the joint. This is where the initiation of joint failure usually occurs, as this is where the joint is subjected to the highest normal stresses. When comparing the experimental and simulation results for 0.1 mm thick joints made with Epidian 57/PAC adhesive, it should be noted that the highest reduced stresses obtained in the simulation results using the multi-zone model are 0.9% higher than the average destructive stresses determined experimentally for the tensile testing of paddle samples. The reduced stresses in the single-zone model are 5.93% lower than the average destructive stresses determined in the experimental test. In many studies, authors point to differences between simulation and experimental results, which often exceed 5%. At this point, it is worth mentioning the standard deviations for the analyzed cases, i.e., for Epidian 57/PAC adhesive: 5.51% and for Epidian 57/Z1 adhesive: 3.81%. The differences in results between the above models reach 7.4%. The comparison between the average destructive stresses should be treated as a kind of model validation, but it should be noted that the presented model does not take into account phenomena related to the adhesion of the adhesive to the substrate, which often determines the destruction of the joint. As a measure of conformity, it can be assumed that the stresses in this area, with the same deformation corresponding to the stress destroying the joint, should take the value closest to the stress destroying the adhesive material. The modified Young's modulus distribution in the adhesive joint may lead to earlier failure initiation. This effect results from stiffness gradients across the bond thickness, which amplify local stress concentrations near the joint edges rather than from a uniform increase in adhesive stiffness. However, it should be noted that both models reproduce quite well the stress levels expected in a stressed adhesive joint. It should be emphasized that the present model isolates the influence of elastic stiffness heterogeneity. Interfacial fracture energy, cohesive damage evolution and potential defect-driven crack initiation were intentionally excluded to avoid conflating material gradient effects with fracture mechanics parameters. Therefore, the observed improvement in stress prediction accuracy can be attributed specifically to stiffness gradient incorporation rather than to enhanced failure modelling complexity. Taking into account changes in Young's modulus at the thickness of the adhesive bond significantly improves the accuracy of predicting its stress and strength. Introducing such heterogeneity into FEM requires only a modification of the material model definition, which can be easily implemented through a user subroutine without significantly increasing computational costs and without the risk of creating artificial stress concentrations. The application of this approach shows that very thin joints, approximately 0.05 mm, achieve greater strength than 0.1 mm joints, which correlates with their higher local Young's modulus. To assess whether the stiffness gradient influences only local stress concentration or also the global structural response, the effective joint stiffness was evaluated from the initial slope of the force–displacement curve. The difference between homogeneous and gradient models did not exceed 2%, indicating that the gradient primarily affects local failure-driving stresses rather than global joint rigidity.

It should be emphasized that the observed influence of through-thickness stiffness gradients is inherently coupled with the stiffness of the adherends. The constraint imposed by relatively rigid substrates governs the development of stress concentrations within the adhesive layer, particularly near the overlap edges where failure initiation is expected. In this context, the presence of a stiffness gradient amplifies local stress variations rather than altering the global

load transfer mechanism. Therefore, the effect identified in this study should be interpreted as a coupled material–structural phenomenon, in which the heterogeneous properties of the adhesive layer interact with the mechanical constraint imposed by the adherends. Consequently, neglecting either the adherend stiffness or the through-thickness variability of adhesive properties may lead to an incomplete representation of the stress state in ultra-thin bonded joints. The present modelling approach ensures that both effects are consistently taken into account within the framework of standardized joint geometry and loading conditions.

The final conclusions indicate that taking into account the increased Young's modulus in thin adhesive joints (below 0.1 mm) can significantly increase the accuracy of numerical calculations. For the design of joints, especially those used in sectors requiring high reliability, it is therefore crucial to take into account the variability of stiffness across the joint cross-section. Although homogeneous models continue to provide satisfactory predictions, the selection of a multi-zone approach should be determined by the level of accuracy required in the analysis. Additional studies are necessary to refine the numerical description of thin adhesive layers and to gain a deeper understanding of how local properties of adhesive layer affect the behaviour of the entire bonded joint. The principal contribution of this work lies in demonstrating that experimentally calibrated through-thickness stiffness gradients measurably alter the failure-driving stress field in ultra-thin adhesive joints, even when global stiffness remains practically unchanged.

References

[1] ADAMS, R.D., WAKE, W.C. (1984). Structural adhesive joints in engineering. Springer Netherlands, Dordrecht.

[2] PN-EN ISO 527-1:2020-01 (2024). Plastics – determination of tensile properties – Part 1: General principles. Polish Committee for Standardization.

[3] KINLOCH, A.J., KODOKIAN, G.A. (1987). The impact resistance of structural adhesive joints. In: *The Journal of Adhesion*, Vol. 24, pp. 109–126.

[4] KINLOCH, A.J., TAIG, C.M. (1987). The adhesive bonding of thermoplastic composites. In: *The Journal of Adhesion*, Vol. 21, pp. 291–302.

[5] KUCZMASZEWSKI, J., ANASIEWICZ, K. (2017). Influence of adhesive layer thickness on joint rigidity in metal-metal butt joints. In: *Assembly Techniques and Technologies*, Vol. 97.

[6] ANASIEWICZ, K., KUCZMASZEWSKI, J. (2019). Adhesive joint stiffness in the aspect of FEM modelling. In: *Materials*, Vol. 12(23), 3911. doi.org/10.3390/ma12233911

[7] ANASIEWICZ, K., KUCZMASZEWSKI, J. (2021). Apparent Young's modulus of the adhesive in numerical modelling of adhesive joints. In: *Materials*, Vol. 14(2), 328. doi.org/10.3390/ma14020328

[8] KEDWARD, K., ZHU, Y., KIEFER, S. (2005). Evaluation of composite bonded joint designs for space applications. In: *46th AIAA/ASME/ASCE/AHS/ASC Structures, Structural Dynamics and Materials Conference*. doi:10.2514/6.2005-2098

[9] KUCZMASZEWSKI, J. (1995). Podstawy konstrukcyjne i technologiczne oceny wytrzymałości adhezyjnych połączeń metali, WUPL, Lublin.

[10] TAIB, A.A., BOUKHILI, R., ACHIOU, S., GORDON, S., BOUKEHILI, H. (2006). Bonded joints with composite adherends. Part I. In: *International Journal of Adhesion and Adhesives*, Vol. 26, pp. 226–236. doi: 10.1016/j.ijadhadh.2005.03.015

[11] DAVIES, P., SOHIER, L., COGNARD, J.-Y., BOURMAUD, A., CHOQUEUSE, D., RINNERT, E., CRÉAC'HCADEC, R. (2009). Influence of adhesive bond line thickness on joint strength. In: *International Journal of Adhesion and Adhesives*, Vol. 29, pp. 724–736. doi: 10.1016/j.ijadhadh.2009.03.002

[12] YAN, C., MAI, Y.-W., YE, L. (2001). Effect of bond thickness on fracture behavior in adhesive joints. In: *The Journal of Adhesion*, 75(1), pp. 27–44. doi: 10.1080/00218460108029592.

[13] PARK, J.-H., CHOI, J.-H., KWEON, J.-H. (2010). Evaluating the strengths of thick aluminum-to-aluminum joints with different adhesive lengths and thicknesses. In: *Composite Structures*, Vol. 92, pp. 2226–2235. doi: 10.1016/j.compstruct.2009.08.037

[14] LEE, D.-B., IKEDA, T., MIYAZAKI, N., CHOI, N.-S. (2002). Damage zone and fracture toughness. In: *Engineering Fracture Mechanics*, Vol. 69, pp. 1363–1375. doi.org/10.1115/1.1417980

[15] ADAMS, R.D., COPPENDALE, J. (1979). Stress–strain behaviour of axially-loaded butt joints. In: *The Journal of Adhesion*, Vol. 10, pp. 49–62.

[16] BYKOV, Y.A., KARPUKHIN, S.D., PANFILOV, Y.V., BOICHENKO, M.K., CHEPTSOV, V.O., OSIPOV, A.V. (2003). Measurement of hardness of thin films. In: *Metal Science and Heat Treatment*, Vol. 45, pp. 396–399. doi.org/10.1023/B:MSAT.0000009788.88059.14

[17] ANASIEWICZ, K., KUCZMASZEWSKI, J. (2016). Pozorny moduł Younga w połączeniach adhezyjnych. In: *Welding Technology Review*, Vol. 88.

[18] BUDZIK, M.K., MASCARO, B., JUMEL, J., CASTAINGS, M., SHANAHAN, M. (2012). Monitoring crosslinking of a DGEBA-PAMAM adhesive in composite/aluminium bonded joint using mechanical and ultra-sound techniques. In: *International Journal of Adhesion and Adhesives*, Vol. 35, pp. 120–128. doi:10.1016/j.ijadhadh.2012.02.009

[19] CARRILLO, F. GUPTA, S., BALOOCH, M., et al. (2005). Nanoindentation of polydimethylsiloxane elastomers: Effect of crosslinking, work of adhesion, and fluid environment on elastic modulus. In: *Journal of Materials Research*, Vol. 20, pp. 2820–2830. doi.org/10.1557/JMR.2005.0354

[20] MASCARO, B. BUDZIK, M. K., CASTAINGS, M., JUMEL, J., SHANAHAN, M. E. R., (2012). Evaluation of adhesive bond modulus. In: *Journal of Physics Conference Series*, Vol. 353, 12006. doi:10.1088/1742-6596/353/1/012006

[21] CZUB, P., PENCZEK, P., BOŃCZA-TOMASZEWSKI, Z., PIELICHOWSKI, J. (2002). Chemia i technologia żywic epoksydowych, WNT, Warszawa.

[22] STAPLETON, S.E., WAAS, A.M., BEDNARCZYK, B.A. (2012). Modelling progressive failure of bonded joints using a single joint finite element. In: *AIAA Journal*, Vol. 49, pp. 1740–1749. doi:10.2514/1.J050889

[23] MAGGIORE, S., BANEA, M.D., STAGNARO, P., LUCIANO, G. (2021). Review of structural adhesive joints in hybrid joining processes. In: *Polymers*, Vol. 13. doi.org/10.3390/polym13223961

[24] GOLAND, M., REISSNER, E. (1944). The stresses in cemented joints. In: *Journal of Applied Mechanics*, Vol. 11, pp. A17–A27.

[25] VOLKERSEN, O. (1938). Die Nietkraftverteilung in zugbeanspruchten Nietverbindungen mit konstanten Laschenquerschnitten. In: *Luftfahrtforschung*, Vol. 15, pp. 41-47.

[26] HART-SMITH, L.J. (1973). Adhesive-bonded double-lap joints, Report/Monograph.

[27] KALINA, T., SEDLÁČEK, F. (2019). Design and determination of strength of adhesive bonded joints. In: *Manufacturing Technology*, Vol. 19(3), pp. 409–413, DOI: 10.21062/ujep/305.2019/a/1213-2489/MT/19/3/409.

[28] KOLAR, V., MULLER, M. (2018). Research on influence of polyurethane adhesive modified by polyurethane filler based on recyclate. In: *Manufacturing Technology*, Vol. 18(3), pp. 418–423. doi: 10.21062/ujep/115.2018/a/1213-2489/MT/18/3/418.

[29] MÜLLER, M. (2013). Research of renovation possibility of machine tools damage by adhesive bonding technology. In: *Manufacturing Technology*, Vol. 13(4), pp. 504-509. doi: 10.21062/ujep/x.2013/a/1213-2489/MT/13/4/504

[30] ŠLEGER, V., MÜLLER, M. (2016). Low-cyclic fatigue of adhesive bonds. In: *Manufacturing Technology*, Vol. 16(5). pp. 1151–1157. doi: 10.21062/ujep/x.2016/a/1213-2489/MT/16/5/1151

[31] CIDLINA, J., MULLER, M., VALASEK, P. (2014). Evaluation of adhesive bond strength depending on degradation type and time. In: *Manufacturing Technology*, Vol. 14(1), pp. 8-12. doi: 10.21062/ujep/x.2014/a/1213-2489/MT/14/1/8

[32] CORRADO, A., POLINI, W. (2024). A unique numerical model to evaluate the influence of adherends' misalignment on adhesive joint strength. In: *Manufacturing Technology*, Vol. 24(2), pp. 183-191. doi: 10.21062/mft.2024.029

[33] ANASIEWICZ, K. (2024). Studies of nanoscratching in the aspect of homogeneity of adhesive joints. In: *Manufacturing Technology*, Vol. 24(6), pp. 150–157. doi: 10.21062/mft.2024.102

[34] ANASIEWICZ, K., KUCZMASZEWSKI, J. (2023). Heterogeneity of adhesive joint properties. In: *Materials*, Vol. 16(23), 7303. doi.org/10.3390/ma16237303

[35] CIECH-SARZYNA (2022). Safety Data Sheet – EPIDIAN® 57. Available at: https://www.polimal.com.pl/wp-content/uploads/2019/02/EPIDIAN_Ciech_Sarzyna.pdf (accessed 2 Dec 2025).

[36] CIECH-SARZYNA (2022). Safety Data Sheet – PAC Hardener. Available at: https://www.zywicesarzyna.pl/produkty/utwardzacz-pac/ (accessed 2 Dec 2025).

[37] CIECH-SARZYNA (2022). Safety Data Sheet – Z1 Hardener. Available at: https://www.zywicesarzyna.pl/produkty/utwardzacz-z1/ (accessed 2 Dec 2025).

[38] LAMBERTI, M., MAUREL-PANTEL, A., LEBON, F. (2023). Experimental characterization and modelling of adhesive bonded joints under static and non-monotonic fracture loading in the mode II regime. *International Journal of Adhesion and Adhesives*, 124, 103394. DOI: 10.1016/j.ijadhadh.2023.103394.

[39] RIES, M. (2024). Mechanical behavior of adhesive joints: A review on modeling techniques. *Computer Methods in Materials Science*, 24(4), pp. 5–35. DOI: 10.7494/cmms.2024.4.1010.

[40] DOBRZAŃSKI, P., OLEKSIAK, W. (2021). Design and analysis methods for composite bonded joints. *Transactions on Aerospace Research*, 2021(1), pp. 45–63. DOI: 10.2478/tar-2021-0004.